quantitation. To the cell pellet, 400 µl of 0.1 N NaOH was added and solubilized, and then a 25-µl aliquot of cell lysate was used to determine protein concentration by the method of Lowry with BSA as a standard. Transport for estradiol-17β-D-glucuronide and estrone-3-sulfate was determined after 3 and 1 min of incubation, periods within which uptake rate was not saturated, with concentrations of 500 nM and 50 nM at 37°C, respectively. The uptake rate was estimated by subtracting uptake by mock cells from total uptake by *SLCO1B1* cDNA-transfected cells and expressed as a percentage of *SLCO1B1*1a* (reference allele). For transport assay of statins, a preliminary study was carried out to estimate IC_{50} values of statins by examining the transporting activity for estradiol-17β-D-glucuronide and estrone-3-sulfate substrate in the absence or presence of various concentrations of statins. IC_{50} values estimated were: approximately 10 µM for atorvastatin and cerivastatin and approximately 100 µM for pravastatin and simvastatin. Thus, the substrate concentrations in the transport medium were set at 20 µM for pravastatin, 0.5 µM for atorvastatin and cerivastatin, and 10 µM for simvastatin so that the substrate concentrations would be lower than those at which half the maximal uptake occurs (K_m). The incubation period for pravastatin was set at 5 min and the incubation periods for atorvastatin, cerivastatin and simvastatin were set at 1 min in order to determine the initial uptake rate. The uptake rate was expressed as cell-to-medium ratio, which was estimated by dividing the amount of statins accumulated in cells by the substrate concentration in the transport medium.

Kinetic analysis

Transport for pravastatin and atorvastatin was determined after 5 and 1 min of incubation with 5, 10, 20, 50 and 100 µM and with 0.5, 2, 5, 20 and 50 µM at 37°C, respectively. The OATP1B1-mediated uptake was calculated after subtracting the uptake by the mock cells from the uptake by *SLCO1B1* cDNA-transfected cells at each concentration. Michaelis–Menten-type nonlinear curve fitting was carried out to obtain kinetic parameters of the maximal uptake rate (V_{max}) and K_m (DeltaGraph 4.5, RockWare Inc., Golden, Colorado, USA).

Analytical procedures for 3-hydroxy-3-methylglutaryl coenzyme A reductase inhibitors (statins)

Quantitation of statins was performed using HPLC tandem mass spectrometry. The HPLC system consisted of three LC-10ADVP pumps, a SLC-10AVP controller, a SIL-HTC auto-injector and a FCV-12AH switching valve (Shimadzu, Kyoto, Japan). The HPLC column used was a CAPCELL PAK C8 UG120 (5 µm in particle size, 4.6 × 35 mm, Shiseido, Tokyo, Japan). Aliquots (pravastatin, 100 µl; atorvastatin, cerivastatin, simvastatin, 10 µl) of samples were injected onto the column with the mobile phase consisting of methylammonium acetate (pH 4.5; 1 mM)-acetonitrile-methanol (70:15:15; v/v/v; eluate C) at a flow rate of 1.2 ml/min. After 1 min, the mobile phase was changed to a mixture of methylammonium acetate (pH 4.5; 1 mM)-acetonitrile-methanol (30:35:35; v/v/v; eluate A) and methylammonium acetate (pH 4.5; 1 mM)-acetonitrile-methanol (10:45:45; v/v/v; eluate B) at a flow rate of 0.5 ml/min using a gradient program described below, and the eluate was taken into the mass spectrometer. After 5 min, the solvent was switched to eluate C to re-equilibrate the column. The time program of the mixture ratio of eluate A and eluate B was set as follows: 0% B for 0–1.2 min, linear gradient from 0 to 100% B for 1.2–3.5 min, 100% B for 3.5–4.7 min, linear gradient from 100 to 0% B for 4.7–4.8 min, and then 0% B for 4.8–7.0 min. The analytes were detected by an API4000 tandem mass spectrometer with a turbo-ion spray interface (Applied Biosystems, Foster, California, USA). All analytes were detected in positive mode, and the precursor to product ions monitored were m/z 447.3 > m/z 327.3 (pravastatin), m/z 559.3 > m/z 440.4 (atorvastatin), m/z 460.3 > m/z 356.1 (cerivastatin), and m/z 441.3 > m/z 325.3 (simvastatin). Samples for calibration, validation and quality control were prepared in a manner similar to that used for preparation of analytical samples described above. Briefly, untransfected HEK293 cells seeded on a 12-well plate were washed three times with ice-cold DMEM, and extraction solution spiked with known amounts of standards was added. Then the following procedures (i.e. extraction and filtration) were carried out. The quantitative range of analytes was determined by intra-day reproducibility assays in which the limit of quantitation was set at 0.25 nM for pravastatin, atorvastatin and cerivastatin and at 2.5 nM for simvastatin, as these were sufficient to estimate the lowest concentrations at which acceptable accuracy ($< 100 \pm 20\%$) and imprecision ($< \pm 20\%$) were obtained.

Immunofluorescence microscopy

Transfected cells were grown on chamber slides (Nalge Nunc International, Naperville, Illinois, USA). Sodium butyrate was added to the culture medium 1 day before the experiment. After washing twice with PBS, the monolayers were fixed with 4% formaldehyde in PBS. After rinsing cells with PBS, the cells were incubated with 0.05% Tween 20 in PBS (PBS-T) containing 3% BSA for 30 min at room temperature for blocking. The monolayers were incubated with the previously described primary antibody against OATP1B1 (1:50-fold in PBS-T) for 1 h at room temperature. Cells were washed four times with PBS-T and then incubated with PBS-T containing goat anti-rabbit IgG labeled with Alexa Fluor 488 (Molecular Probes, Inc., Eugene, Oregon, USA) for 1 h at room temperature. After washing cells twice with PBS-T, about two drops of ProLong Antifade reagent/mounting mixture (Molecular Probes) were added to the slide. Confocal laser-scanning immunofluorescence microscopy was performed using FluorView FV-500 (Olympus, Tokyo, Japan).

Results

Expression of SLCO1B1 in HEK293 and HeLa cells

Levels of OATP1B1 mRNA transiently expressed in HEK293 and HeLa cells were analyzed by RT–PCR. As shown in Fig. 1, the levels of mRNA were apparently equal among OATP1B1*1a and variants in either of HEK293 or HeLa cells.

Transport activity of SLCO1B1 allelic variants for typical substrates

The relative transporting activities of the *SLCO1B1* variants for estradiol-17β-D-glucuronide and estrone-3-sulfate are shown in Fig. 2. The transporting activities for these typical substrates of OATP1B1 significantly decreased in either HEK293 and HeLa cells expressing *SLCO1B1*5*, *15, *5 + C1007G* and *15 + C1007G*. The extents of decrease were not greatly different among these variants, ranging from −37% to −73% of that of *SLCO1B1*1a*. In contrast, there was no apparent tendency of changes in the activities of cells expressing *SLCO1B1*1b*, *1a + C1007G* and *1b + C1007G*, which ranged from 85% to 130% of that of *SLCO1B1*1a*.

Transport activity of OATP1B1 allelic variants for statins

Since the effects of OATP1B1 variants on activities for the uptake of typical substrates of OATP1B1 were similar in HEK293 and HeLa cells, the effects of these valiant alleles on the transport of statins were studied using only HEK293 cells. Similar to the results for typical substrates of OATP1B1, transporting activities for pravastatin, atorvastatin and cerivastatin decreased significantly in HEK293 cells expressing *SLCO1B1*5, *15, *5 + C1007G* and *15 + C1007G*, whereas those of *SLCO1B1*1b, *1a + C1007G* and *1b + C1007G* were not apparently different from that of *SLCO1B1*1a* (Fig. 3a–c). However, the extents of decreases in the activities of cells expressing *SLCO1B1*5, *15, *5 + C1007G* and *15 + C1007G* appeared to be different among statins when they were compared with the activity of *SLCO1B1*1a*.

Fig. 1

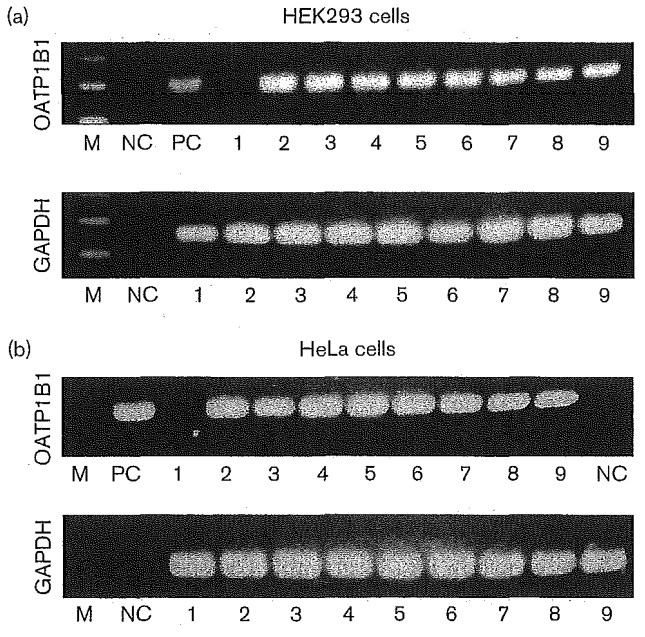

RT–PCR analysis of mRNA expression of (a) OATP1B1 and GAPDH in HEK293 cells and (b) OATP1B1 and GAPDH in HeLa cells transiently expressing *SLCO1B1* allelic variants. Specific bands corresponding to OATP1B1 and GAPDH are shown with sizes of 194 and 177 base pairs, respectively. M, marker; NC, negative control; PC, positive control; 1, mock; 2, OATP1B1*1a; 3, OATP1B1*1b; 4, OATP1B1*5; 5, OATP1B1*15; 6, OATP1B1*1a+C1007G; 7, OATP1B1*1b+C1007G; 8, OATP1B1*5+C1007G; 9, OATP1B1*15+C1007G.

Fig. 2

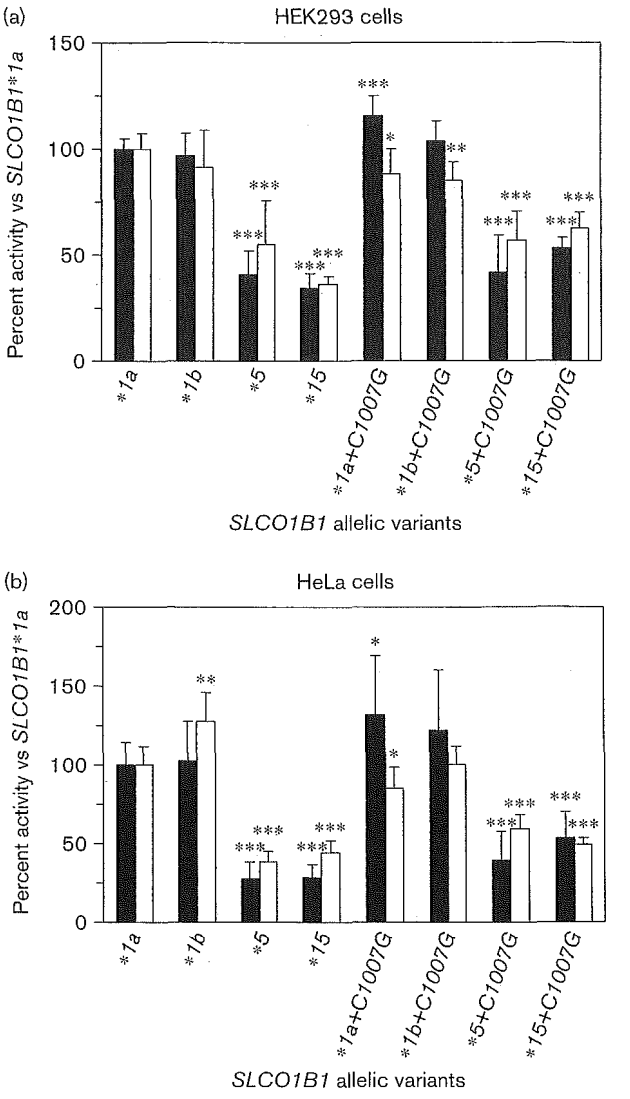

Uptake of [^{3}H]estradiol-17β-glucuronide (closed bars) and [^{3}H]estrone-3-sulfate (open bars) into (a) HEK293 cells and (b) HeLa cells transiently expressing *SLCO1B1* allelic variants. Each bar represents the mean and S.D. of three independent assays. *$P<0.05$, **$P<0.01$, ***$P<0.001$ significantly different from the uptake by *SLCO1B1*1a*.

Fig. 3

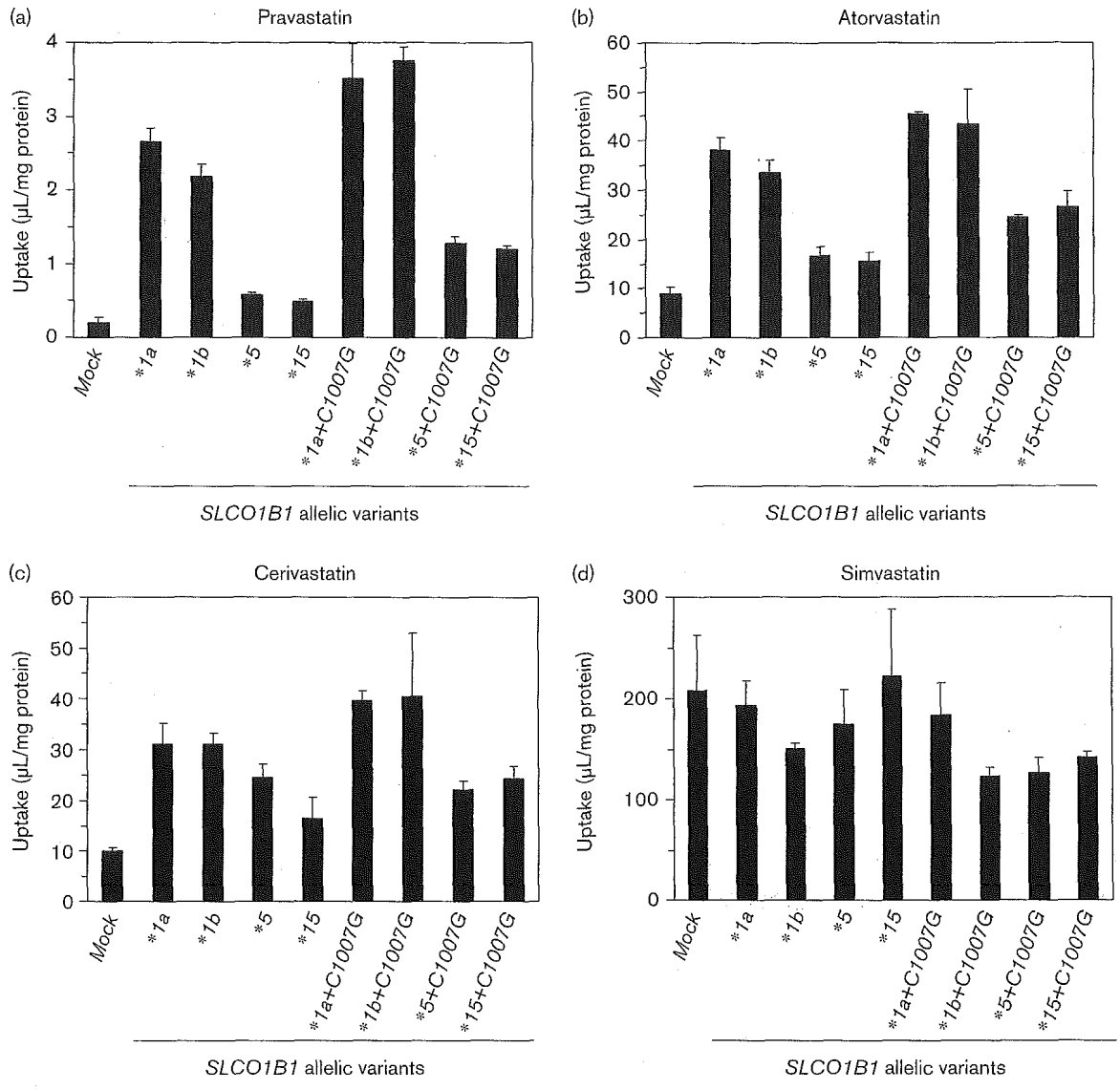

Uptake of statins into HEK293 cells transiently expressing *SLCO1B1* allelic variants. (a) pravastatin, (b) atorvastatin, (c) cerivastatin, and (d) simvastatin. Each bar represents the mean and S.D. of triplicated determinations.

The most prominent decrease was found for pravastatin followed by atorvastatin and cerivastatin. In contrast, a tendency of decreases such as that found in the typical substrates and the three statins was not observed for simvastatin, for which the activities of cells expressing *SLCO1B1*5* and **15* were not different from that of *SLCO1B1*1a* and those of *SLCO1B1*1a* and its variants were comparable or less than that of mock (Fig. 3d).

Kinetic analysis

Since the effects of *SLCO1B1*5*, **15* and **15 + C1007G* on the transporting activity of OATP1B1 for statins were most prominent for pravastatin and atorvastatin, the effects of *SLCO1B1*1b*, **5*, **15* and **15 + C1007G* on the kinetics of these statins were studied using HEK293 cells. As shown in Fig. 4, saturable transport was observed for both statins. The kinetic parameters estimated are summarized in Table 2. Although the differences were not so apparent for K_m values of these statins among the five haplotypes studied, the V_{max} values of cells expressing *SLCO1B1*5*, **15* and **15 + C1007G* were significantly lower than that of *SLCO1B1*1a*. Accordingly, intrinsic clearance (V_{max}/K_m) of pravastatin and atorvastatin decreased by 79%, 80% and 61% and by 67%, 60% and 66% for *SLCO1B1*5*, **15* and **15 + C1007G*, respectively, as compared to *SLCO1B1*1a*.

Table 2 Kinetic parameters of pravastatin and atorvastatin uptake by *SLCO1B1* allelic variants

Substrate	*SLCO1B1* allelic variants	*N*	K_m(μM)	V_{max}(pmol/min/mg)	V_{max}/K_m(μl/min/mg)
Pravastatin					
	*1a	5	85.7±29.8	58.2±4.1	0.753±0.291
	*1b	5	88.7±20.6	61.0±19.0	0.722±0.263
	*5	5	153±80	22.4±9.0***	0.155±0.022*
	*15	4	118±69	17.0±8.1***	0.154±0.030*
	*15+C1007G	5	145±38*	40.8±5.2***	0.294±0.073*
Atorvastatin					
	*1a	4	12.4±4.8	70.4±29.9	5.65±0.95
	*1b	4	12.7±4.5	59.3±10.5	5.01±1.22
	*5	3	11.1±7.6	16.0±4.3*	1.88±1.16**
	*15	3	9.29±2.83	19.2±2.4*	2.28±1.08**
	*15+C1007G	3	13.1±6.1	23.3±7.4*	1.91±0.59**

N means numbers of assays;
*$P<0.05$,
**$P<0.01$,
***$P<0.001$ significantly different from the uptake by *SLCO1B1*1a*.

Cell surface expression of OATP1B1 allelic variants

Since *SLCO1B1* allelic variants did not alter either the mRNA levels or K_m values of statins, the decrease in intrinsic clearance could be derived from the reduced level of functional OATP1B1 protein in the plasma membrane. Accordingly, immunocytochemical analysis was performed to examine the cellular localization of OATP1B1 variants. Fig. 5 shows the staining of OATP1B1 proteins in HEK293 cells transfected with *SLCO1B1*1a*, *1b*, *5*, *15*, *15+C1007G* and mock vectors. *SLCO1B1*1a* and *1b* allelic proteins were mainly localized at the plasma membrane, whereas *SLCO1B1*5*, *15* and *15+C1007G* allelic proteins were observed both in the intracellular space and at the plasma membrane. Similar results were also obtained for HeLa cells transfected with vectors of these *SLCO1B1* allelic variants (data not shown).

Discussion

The results of the present study clearly showed that the transporting activities of OATP1B1 for its typical substrates, estradiol-17β-D-glucuronide and estrone-3-sulfate, and for three statins, pravastatin, atorvastatin and cerivastatin, decreased significantly in HEK293 and/or HeLa cells expressing *SLCO1B1*5, *15, *5+C1007G* and *15+C1007G*, whereas those of *SLCO1B1*1b, *1a+C1007G* and *1b+C1007G* were not apparently different from those of *SLCO1B1*1a* (Figs 2, 3 and 4). Since *SLCO1B1*5* contains 521T>C and *SLCO1B1*15* contains both of 388A>G and 521T>C, the results suggest that 521T>C is the key SNP for determining the functional alteration of OATP1B1. This contention is in good agreement with the present findings that *SLCO1B1*5, *15* and *15+C1007G* allelic proteins are localized not only at the plasma membrane but also in the intracellular space in both HeLa cells and HEK293 cells, suggesting that decreased activities of cells expressing *SLCO1B1*5, *15* and *15+C1007G* are mainly and commonly derived from a sorting error caused by 521T>C that substitutes a valine to an alanine residue at position 174 in OATP1B1, which is putatively located on transmembrane-spanning domain 4 [8].

The present in-vitro findings are consistent with previous in-vivo observations that the area under the plasma concentration–time curve (AUC) of pravastatin was significantly greater in carriers of the haplotype of *SLCO1B1*5* or *15* than that of *SLCO1B1*1a* or *1b* [12,14,16]. However, the extent of decrease in the transporting capacity of OATP1B1 by the mutation of *SLCO1B1*5* and *15 in vivo* is difficult to assess because information on non-renal clearance of pravastatin in homozygote of *SLCO1B1*5* or *15* is limited. However, the value of pravastatin reported in one subject who is homozygous for *SLCO1B1*15* was 86 to 87% lower and those in heterozygotes of *SLCO1B1*15* were 45 to 50% lower than those in homozygotes of *SLCO1B1*1a* or *1b* [14]. These values are in good agreement with or explainable by the results of the present study showing that V_{max}/K_m of pravastatin uptake in HEK293 cells expressing *SLCO1B1*15* was 80% and 79% lower than those of *SLCO1B1*1a* and *1b*, respectively (Table 2).

Contradicting results have been reported for the influence of *SLCO1B1*5* on the function of OATP1B1 in cDNA-expression systems in which transporting activities of cells expressing *SLCO1B1*5* for estradiol-17β-D-glucuronide and estrone-3-sulfate were reduced to less than half of those of *SLCO1B1*1a* when they were transiently expressed in HeLa cells [8], whereas the activities for estrone-3-sulfate were not different between *SLCO1B1*5* and *1a* in HEK293 cells [13]. The results of the present study showed that transporting activities of *SLCO1B1*5* allelic protein decreased to less than or around 50% of those of *SLCO1B1*1a* for both 17β-D-glucuronide and estrone-3-sulfate in HeLa cells and even in HEK293 cells, being consistent with results reported by Tirona *et al.* [8]. Therefore, the capacity of

Fig. 4

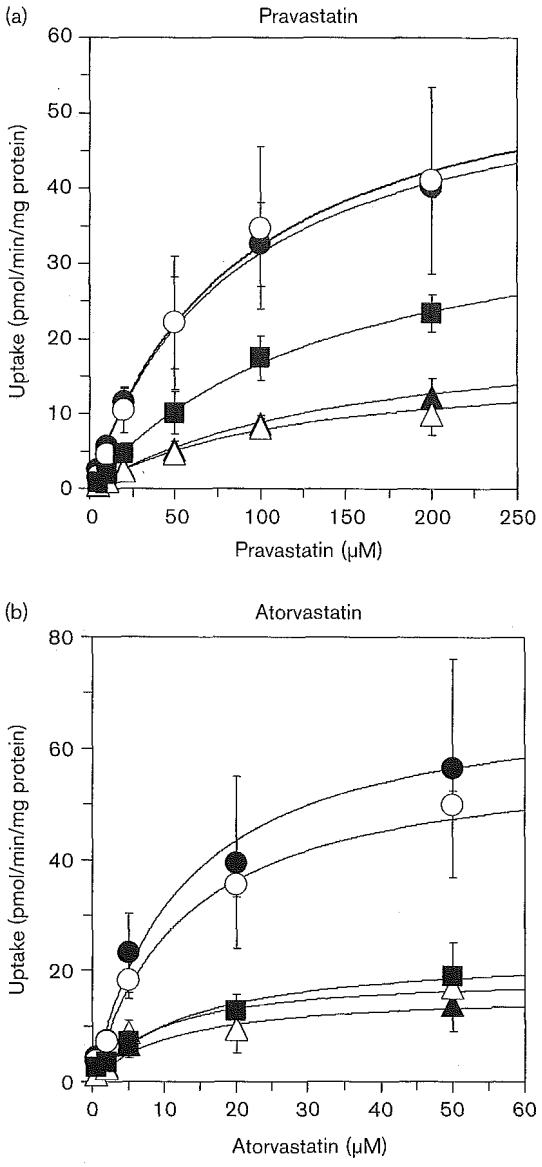

Concentration dependence of (a) pravastatin and (b) atorvastatin uptake into HEK293 cells transiently expressing *SLCO1B1*1a* (closed circles), **1b* (open circles), **5* (closed triangles), **15* (open triangles) or **15+C1007G* (closed squares). Each value is the mean ± SD of at least three independent assays, and the solid lines represent the results of nonlinear least-squares analysis.

Fig. 5

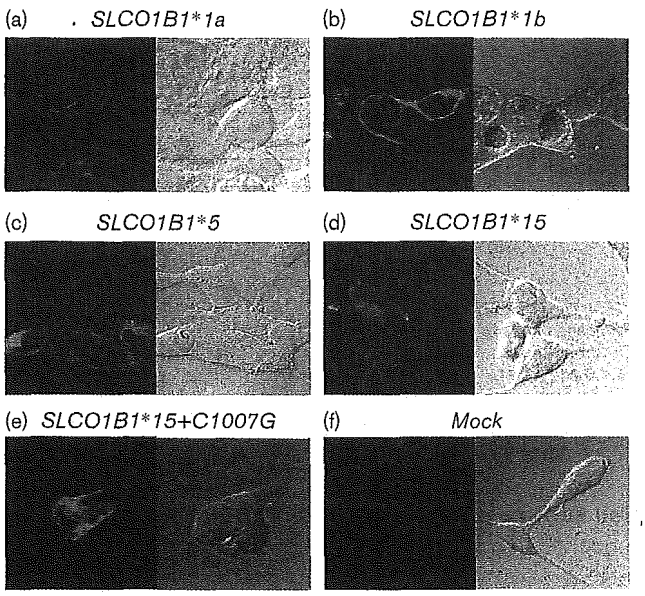

Immunolocalization of (a) *SLCO1B1*1a*, (b) *SLCO1B1*1b*, (c) *SLCO1B1*5*, (d) *SLCO1B1*15*, (e) *SLCO1B1*15+C1007G* allelic proteins, and (f) mock in HEK293 cells. Fluorescent images are shown on the left, and phase contrast images are shown on the right.

*SLCO1B1*5* allelic protein is considered to be decreased both *in vitro* [8] and *in vivo* [12,14,16], although it remains unknown why there were contradicting findings in previous studies. It is possible that such characteristics were altered by maintenance conditions such as additional chemicals used for transfection or sodium butyrate.

The results of the present study showed that 388A > G did not alter the activity of OATP1B1 significantly. This contradicts the finding reported by Mwinyi *et al.* [12] that the AUC of pravastatin was 60% smaller in subjects carrying *SLCO1B1*1b* than that in homozygous subjects of **1a*, suggesting that uptake of pravastatin by OATP1B1 is increased by 388A > G. Nonetheless, our findings are consistent with results of three independent in-vitro studies [8,13,17] and one in-vivo study showing that **1b* does not affect the activity of OATP1B1 [14]. Therefore, it is conceivable that 388A > G does not alter the transporting activity of OATP1B1 at least when pravastatin is used as a substrate, although further in-vivo study is needed to confirm our and others' in-vitro findings [8,13,17]. The present results also suggest that 1007C > G does not influence the activity of OATP1B1 dramatically, although it substitutes a proline to an arginine residue at position 336 in OATP1B1 that is putatively located on transmembrane-spanning domain 7. It is notable that 1007C > G is the first example of a nonsynonymous SNP that does not appear to affect the function of OATP1B1 despite its localization on a transmembrane-spanning domain. All of the mutations localized on the putative transmembrane-spanning domain of OATP1B1 reported previously are associated with significant reduction in their transporting activities [8].

Of the four statins studied, the most prominent decrease in the activities of cells expressing *SLCO1B1*5* or **15* was found for pravastatin followed by atorvastatin and cerivastatin, but no apparent decrease was found for simvastatin when the activities were compared with

*SLCO1B1*1a* (Fig. 3). This tendency may be explained by the physicochemical properties of statins. The water/octanol partition coefficients of pravastatin, atorvastatin, cerivastatin and simvastatin have been reported to be −0.47, 1.53, 2.32 and 4.40, respectively [18], which are in the same order as that of less decreases in the activities for statins. This phenomenon appears to be derived from the extent to which OATP1B1 contributes to the total transmembrane distribution of statins that includes passive diffusion. Comparing the uptake rates in mock among these statins, which would express the sum of passive diffusion and active transport in a background, the uptake rate of simvastatin was about 20-fold higher than that of atorvastatin and cerivastatin and about 2000-fold higher than that of pravastatin. These findings indicate that the transporting activity of OATP1B1 for simvastatin is much less than the passive diffusion because of its high lipophilicity. On the other hand, atorvastatin and cerivastatin are transported in part by passive diffusion because of their moderate lipophilicity, while pravastatin is not transported extensively by passive diffusion because of its hydrophilicity. Thus, it is thought that the uptake of pravastatin is affected remarkably and the uptake of atorvastatin and cerivastatin is affected moderately by mutations carrying 521T > C. However, further in-vivo studies are clearly needed to confirm these contentions because these findings were derived from an in-vitro study and may not reflect the activity of OATP1B1 *in vivo*.

The present study showed that the uptake clearances (V_{max}/K_m) of atorvastatin and pravastatin decreased to 20 to 40% of cells expressing *SLCO1B1*1a* and that the uptake of cerivastatin at a fixed concentration also decreased to 31 to 69% of *SLCO1B1*1a* in the variants of *SLCO1B1* carrying 521T > C. Since the allele frequencies of *SLCO1B1*5* have been reported to be 14%, 2% and 0.7% in European-American, African-American and Japanese, respectively [8,13] and those of *SLCO1B1*15* have been reported to be 10 to 15% in Japanese [13,14], homozygous of T521C is estimated to exist in at least one of 40 to 50 of European-Americans and Japanese. These findings suggest that 521T > C is a major factor influencing the disposition and even efficacy or adverse reactions of drugs transported by OATP1B1. For example, it is possible that *SLCO1B1*5* and **15* may be one of the risk factors attaining adverse drug reactions such as myopathy or rhabdomyolysis due to statins which has been reported to be dependent on the plasma concentration of statins [19]. In this regard, the possibility that an acid form of simvastatin that is an active form of simvastatin could be transported by OATP1B1 should be noted, although the results of the present study suggest that simvastatin (lactone form) is not efficiently taken up by OATP1B1. Further study is needed to clarify the effect of polymorphisms on transporting activity of OATP1B1 for the acid form of simvastatin. In addition, contribution of other transporters such as OATP1B3 and OATP2B1 should be considered to estimate the effect of SNPs in the *SLCO1B1* on hepatic clearance of drugs *in vivo*.

In conclusion, the results of current study suggest that T521C is the key SNP that causes a sorting error of OATP1B1 and decreases the functional activity of variant proteins derived from *SLCO1B1*5, *15* and **15 + C1007G*.

Acknowledgements

We thank Dr Y. Nakayama (Department of Molecular Biology) for his helpful suggestions in the immunocytochemical study and Dr T Furihata and Mr T Ohishi (Laboratory of Pharmacology and Toxicology, Graduate School of Pharmaceutical Sciences, Chiba University) for their assistance to conduct additional experiments to prepare revised manuscript. We appreciate Dr Takashi Ishizaki (Faculty of Pharmaceutical Sciences, Teikyo Heisei University) for his critical reading and valuable suggestions to prepare this manuscript. We also appreciate Sankyo Co. (Tokyo, Japan) for providing statins.

References

1 Kusuhara H, Sugiyama Y. Role of transporters in the tissue-selective distribution and elimination of drugs: transporters in the liver, small intestine, brain and kidney. *J Control Rel* 2002; **78**:43–54.

2 Abe T, Kakyo M, Tokui T, Nakagomi R, Nishio T, Nakai D, *et al.* Identification of a novel gene family encoding human liver-specific organic anion transporter LST-1. *J Biol Chem* 1999; **274**:17159–17163.

3 Hsiang B, Zhu Y, Wang Z, Wu Y, Sasseville V, Yang WP, *et al.* A novel human hepatic organic anion transporting polypeptide (OATP2). *J Biol Chem* 1999; **274**:37161–37168.

4 Tirona RG, Kim RB. Pharmacogenomics of organic anion-transporting polypeptides (OATP). *Adv Drug Deliv Rev* 2002; **54**:1343–1352.

5 Tamai I, Nezu J, Uchino H, Sai Y, Oku A, Shimane M, *et al.* Molecular identification and characterization of novel members of the human organic anion transporter (OATP) family. *Biochem Biophys Res Commun* 2000; **273**:251–260.

6 Cui Y, Konig J, Leier I, Buchholz U, Keppler D. Hepatic uptake of bilirubin and its conjugates by the human organic anion transporter SLC21A6. *J Biol Chem* 2001; **276**:9626–9630.

7 Kullak-Ublick GA, Ismair MG, Stieger B, Landmann L, Huber R, Pizzagalli F, *et al.* Organic anion-transporting polypeptide B (OATP-B) and its functional comparison with three other OATPs of human liver. *Gastroenterology* 2001; **120**:525–533.

8 Tirona RG, Leake BF, Merino G, Kim RB. Polymorphisms in OATP-C: identification of multiple allelic variants associated with altered transporting activity among European- and African-Americans. *J Biol Chem* 2001; **276**:35669–35675.

9 Tirona RG, Leake BF, Wolkoff AW, Kim RB. Human organic anion transporting polypeptide-C (SLC21A6) is a major determinant of rifampicin-mediated pregnane X receptor activation. *J Pharmacol Exp Ther* 2003; **304**:223–228.

10 Shitara Y, Itoh T, Sato H, Li AP, Sugiyama Y. Inhibition of transporter-mediated hepatic uptake as a mechanism for drug–drug interaction between cerivastatin and cyclosporin A. *J Pharmacol Exp Ther* 2003; **304**:610–616.

11 Schneck DW, Birmingham BK, Zalikowski JA, Mitchell PD, Wang Y, Martin PD, *et al.* The effect of gemfibrozil on the pharmacokinetics of rosuvastatin. *Clin Pharmacol Ther* 2004; **75**:455–463.

12 Mwinyi J, Johne A, Bauer S, Roots I, Gerloff T. Evidence for inverse effects of OATP-C (SLC21A6) 5 and 1b haplotypes on pravastatin kinetics. *Clin Pharmacol Ther* 2004; **75**:415–421.

13 Nozawa T, Nakajima M, Tamai I, Noda K, Nezu J, Sai Y, *et al.* Genetic polymorphisms of human organic anion transporters OATP-C (SLC21A6) and OATP-B (SLC21A9): allele frequencies in the Japanese population and functional analysis. *J Pharmacol Exp Ther* 2002; **302**:804–813.

14 Nishizato Y, Ieiri I, Suzuki H, Kimura M, Kawabata K, Hirota T, *et al.* Polymorphisms of OATP-C (SLC21A6) and OAT3 (SLC22A8) genes: consequences for pravastatin pharmacokinetics. *Clin Pharmacol Ther* 2003; **73**:554–565.

15 Tamai I, Nozawa T, Koshida M, Nezu J, Sai Y, Tsuji A. Functional characterization of human organic anion transporting polypeptide B (OATP-B) in comparison with liver-specific OATP-C. *Pharm Res* 2001; **18**: 1262–1269.

16 Niemi M, Schaeffeler E, Lang T, Fromm MF, Neuvonen M, Kyrklund C, *et al.* High plasma pravastatin concentrations are associated with single nucleotide polymorphisms and haplotypes of organic anion transporting polypeptide-C (OATP-C, SLCO1B1). *Pharmacogenetics* 2004; **14**: 429–440.

17 Michalski C, Cui Y, Nies AT, Nuessler AK, Neuhaus P, Zanger UM, *et al.* A naturally occurring mutation in the SLC21A6 gene causing impaired membrane localization of the hepatocyte uptake transporter. *J Biol Chem* 2002; **277**:43058–43063.

18 Matsuyama K, Nakagawa K, Nakai A, Konishi Y, Nishikata M, Tanaka H, *et al.* T. Evaluation of myopathy risk for HMG-CoA reductase inhibitors by urethane infusion method. *Biol Pharm Bull* 2002; **25**:346–350.

19 Thompson PD, Clarkson P, Karas RH. Statin-associated myopathy. *JAMA* 2003; **289**:1681–1690.

Drug Metab. Pharmacokinet. 20 (2): *SNP13* (144)-*SNP20* (151) (2005).

SNP Communication

Genetic Variations and Haplotypes of UGT1A4 in a Japanese Population

Mayumi SAEKI[1], Yoshiro SAITO[1,2,*], Hideto JINNO[1,3], Kimie SAI[1,4], Akiko HACHISUKA[2], Nahoko KANIWA[1,5], Shogo OZAWA[1,6], Manabu KAWAMOTO[7], Naoyuki KAMATANI[7], Kuniaki SHIRAO[8], Hironobu MINAMI[9], Atsushi OHTSU[10], Teruhiko YOSHIDA[11], Nagahiro SAIJO[12], Kazuo KOMAMURA[13,14], Takeshi KOTAKE[15], Hideki MORISHITA[15], Shiro KAMAKURA[13], Masafumi KITAKAZE[13], Hitonobu TOMOIKE[13] and Jun-ichi SAWADA[1,2]

[1]*Project Team for Pharmacogenetics,* [2]*Division of Biochemistry and Immunochemistry,* [3]*Division of Environmental Chemistry,* [4]*Division of Xenobiotic Metabolism and Disposition,* [5]*Division of Medicinal Safety Science,* [6]*Division of Pharmacology, National Institute of Health Sciences, Tokyo, Japan* [7]*Division of Genomic Medicine, Department of Advanced Biomedical Engineering and Science, Tokyo Women's Medical University, Tokyo, Japan* [8]*Division of Internal Medicine, National Cancer Center Hospital,* [11]*Genetics Division, National Cancer Center Research Institute, National Cancer Center, Tokyo, Japan* [9]*Division of Oncology/Hematology,* [10]*Division of GI Oncology/Digestive Endoscopy,* [12]*Deputy Director, National Cancer Center Hospital East, Chiba, Japan* [13]*Division of Cardiology,* [14]*Department of Cardiovascular Dynamics Research Institute,* [15]*Department of Pharmacy, National Cardiovascular Center, Osaka, Japan*

Full text of this paper is available at http://www.jssx.org

Summary: Nineteen genetic variations, including 11 novel ones, were found in exon 1 and its flanking region of the UDP-glucuronosyltransferase (UGT) 1A4 gene from 256 Japanese subjects, consisting of 60 healthy volunteers, 88 cancer patients and 108 arrhythmic patients. These variations include −217T>G and −36G>A in the 5′-flanking region, 30G>A (P10P), 127delA (43fsX22; frame-shift from codon 43 resulting in the termination at the 22nd codon, codon 65), 175delG (59fsX6), 271C>T (R91C), 325A>G (R109G), and 357T>C (N119N) in exon 1, and IVS1+1G>T, IVS1+98A>G and IVS1+101G>T in the following intron. Among them, 127delA and 175delG can confer early termination of translation, resulting in an immature protein that probably lacks enzymatic activity. Variation IVS1+1G>T is located at a splice donor site and thus may lead to aberrant splicing. Since we did not find any significant differences in the frequencies of all the variations among the three subject groups, the data were analyzed as one group. The allele frequencies of the novel variations were 0.006 for IVS1+101G>T, 0.004 for 30G>A (P10P) and 357T>C (N119N), and 0.002 for the 8 other variations. In addition, the two known nonsynonymous single nucleotide polymorphisms (SNPs), 31C>T (R11W) and 142T>G (L48V), were found at 0.012 and 0.129 frequencies, respectively. The SNP 70C>A (P24T), mostly linked with 142T>G (L48V) in German Caucasians, was not detected in this study. Sixteen haplotypes were identified or inferred, and some haplotypes were confirmed by cloning and sequencing. It was shown that most of 142T>G (L48V) was linked with −219C>T, −163G>A, 448T>C (L150L), 804G>A (P268P), and IVS1+43C>T, comprising haplotype **3a*; haplotype **4a* harbors 31C>T (R11W); 127delA (43fsX22) and 142T>G (L48V) were linked (haplotype **5a*); 175delG (59fsX6) was linked with 325A>G (R109G) (**6a* haplotype); and −219C>T, −163G>A, 142T>G (L48V), 271C>T (R91C), 448T>C (L150L), 804G>A (P268P), and IVS1+43C>T comprised haplotype **7a*. Our results provide fundamental and useful information for genotyping *UGT1A4* in the Japanese and probably Asian populations.

Key words: UGT1A4; amino acid alteration; frameshift; splice donor site; drug metabolism

Received; December 6, 2004, Accepted; February 17, 2005

To whom correspondence should be addressed: Yoshiro SAITO, Ph.D., *Project Team for Pharmacogenetics, National Institute of Health Sciences, 1-18-1 Kamiyoga, Setagaya-ku, Tokyo 158-8501, Japan. Tel. +81-3-3700-9453, Fax. +81-3-3707-6950, E-mail: yoshiro@nihs.go.jp*

Table 1. Primers utilized for *UGT1A4* amplification and sequencing

	Direction	Primer Name	Sequences	Location[a]
Amplification	forward	UGT1A4-1stF	TTAACAAAGTAGAAGGCAGTG	135092
	reverse	UGT1A4-1stR	TGAAAACTTGAAATACACTAGGC	136460
Sequencing	forward	UGT1A4-1stF	TTAACAAAGTAGAAGGCAGTG	135092
	forward	UGT1A4seqF2	GGGCTGAGAGTGGAAAGGT	135502
	forward	UGT1A4seqF3	TCCTTCCTCCTATATTCCTAAGTT	135995
	reverse	UGT1A4seqR1-2	ATCAAATTCCTTCTGGGTCC	135698
	reverse	UGT1A4seqR2	AAGGGGCAGAAAAAGTATGG	136119
	reverse	UGT1A4-1stR	TGAAAACTTGAAATACACTAGGC	136460

[a]The 5′-end of each primer on AF297093.1.

On December 2, 2004, these variations were not found on the UDP Glucuronosyltransferase home page (http://som.flinders.edu.au/FUSA/ClinPharm/UGT/), the Japanese Single Nucleotide Polymorphisms (JSNP) (http://snp.ims.u-tokyo.ac.jp/), dbSNP in the National Center for Biotechnology Information (http://www.ncbi.nlm.nih.gov/SNP/), or PharmGKB (http://www.pharmgkb.org/do/) databases.

This study was supported by the Program for the Promotion of Fundamental Studies in Health Sciences (MPJ-1, -3, and -6) of the Pharmaceuticals and Medical Devices Agency (PMDA) of Japan, and the program for the Promotion of Studies in Health Scrences of the Ministry of Health, Labor and Welfare of Japan.

Introduction

As phase II enzymes, the UDP-glucuronosyltransferase enzymes (UGTs) play crucial roles in the detoxification and elimination of a large number of endogenous and exogenous compounds.[1] Of the UGT1 and UGT2 subfamilies expressed in humans, the genes encoding UGT1As have a unique genetic structure consisting of at least 13 different exon 1′s, including four inactive ones, and the common exons 2 to 5 clustered on chromosome 2q37.[2] One of the exon 1′s can be spliced on to the common exons. The *N*-terminal domains (encoded by the exon 1′s) of the UGT1A proteins determine their substrate-binding specificity, and the common *C*-terminal domain (encoded by exons 2 to 5) is important for UDP-glucuronic acid binding.[3]

UGT1A4 is expressed in the liver, bile ducts, colon, small intestine, and pancreas.[1,4,5] UGT1A4 catalyzes the conjugation of exogenous amines and alcohols, including nicotine, sapogenins, imipramine, trifluoperazine, and tamoxifen.[1,6–9] In addition, many androgens and progestins are reported as endogenous substrates of UGT1A4.[6] Several genetic polymorphisms of *UGT1A4* were reported in the public databases. Among them, two nonsynonymous single nucleotide polymorphisms (SNPs), 70C>A (P24T) and 142T>G (L48V), were found in German Caucasians, and they were shown to be closely associated.[10] The variant enzymes (24T and 48V) had reduced *in vitro* activities for β-naphtylamine, benzidine, *trans*-androsterone, and dihydrotestosterone in a substrate-specific manner.[10]

In spite of the clinical importance of UGT1A4, there is no report on the comprehensive sequencing analysis for the genetic polymorphisms of *UGT1A4* in Asian populations, including the Japanese. In the present study, *UGT1A4* exon 1 was sequenced from 256 Japanese subjects. Eleven novel genetic variations were identified, including 4 nonsynonymous ones.

Materials and Methods

Human genomic DNA samples: DNA was obtained from the blood leukocytes of 88 Japanese cancer patients and 108 Japanese arrhythmic patients. Written informed consent was obtained from all participating patients. DNA was also extracted from Epstein-Barr virus-transformed lymphoblastoid cells, for which blood samples were collected from 60 healthy Japanese volunteers at the Tokyo Women's Medical University under the auspices of the Pharma SNP Consortium (Tokyo, Japan). Informed consent was also obtained from all healthy subjects. The ethical review boards of all the participating organizations approved this study.

PCR conditions for DNA sequencing: First, exon 1 of *UGT1A4* was amplified from genomic DNA (100 ng) using 0.625 units of *Ex*-Taq (Takara Bio. Inc., Shiga, Japan) with 0.2 μM of amplification primers designed in the introns (**Table 1**). The PCR conditions were 94°C for 5 min, followed by 30 cycles of 94°C for 30 sec, 55°C for 1 min, and 72°C for 2 min, and then a final extension at 72°C for 7 min. These PCR products were then treated with a PCR Product Pre-Sequencing Kit (USB Co., Cleveland, OH, USA) and were directly sequenced on both strands using an ABI Big Dye Terminator Cycle Sequencing Kit (Applied Biosystems, Foster City, CA, USA) (see **Table 1** for sequencing primers). The excess dye was removed by a DyeEx96 kit (Qiagen, Hilden, Germany). The eluates were analyzed on an ABI Prism 3700 DNA Analyzer (Applied Biosystems). All variations were confirmed by repeating

Table 2. Summary of *UGT1A4* polymorphisms detected in a Japanese population

SNP ID				Position			Nucleotide change and flanking sequences (5′ to 3′)	Amino acid change	Number of subjects			Frequency			
This Study	dbSNP-NCBI database	JSNP database	Pharm GKB atabase[b]	Location	AF297093.1	From the translational initiation site or from the end of exon 1 (IVS1+)			Wild-type	Hetero-zygote	Homo-zygote	Total (n=256)	Healthy volunteers (n=60)	Cancer patients (n=88)	Arrhythmic patients (n=108)
MPJ6_U1A081	rs3732219	IMS-JST085729	O	5′-flanking	135210	−219	GGGTCAGATGAGC/TTTTTCAAGATAG		195	54	7	0.133	0.133	0.142	0.125
MPJ6_U1A082[a]				5′-flanking	135212	−217	GTCAGATGAGCTT/GTTCAAGATAGGC		255	1	0	0.002	0.000	0.000	0.005
MPJ6_U1A083	rs3732218	IMS-JST085728	O	5′-flanking	135266	−163	TAACGAAAGGCAG/ATTATAGATTAAT		195	54	7	0.133	0.133	0.142	0.125
MPJ6_U1A084[a]				5′-flanking	135393	−36	CAGGCACAGCGTG/AGGGTGGACAGTC		255	1	0	0.002	0.000	0.006	0.000
MPJ6_U1A085[a]				Exon 1	135458	30	GGTTCCCCTGCCG/ACGGCTGGCCACA	P10P	254	2	0	0.004	0.000	0.000	0.009
MPJ6_U1A086	rs3892221		O	Exon 1	135459	31	GTTCCCCTGCCGC/TGGCTGGCCACAG	R11W	250	6	0	0.012	0.025	0.011	0.005
MPJ6_U1A087[a]				Exon 1	135555	127	AGCCCCTGGCTCA/-GCATGCGGGAGG	43fsX22	255	1	0	0.002	0.000	0.000	0.005
MPJ6_U1A088	rs2011425		O	Exon 1	135570	142	ATGCGGGAGGCCT/GTGCGGGAGCTCC	L48V	197	52	7	0.129	0.133	0.148	0.111
MPJ6_U1A089[a]				Exon 1	135603	175	GGCCACCAGGCGG/-TGGTCCTCACCC	59fsX6	255	1	0	0.002	0.000	0.000	0.005
MPJ6_U1A090[a]				Exon 1	135699	271	AAGGAATTTGATC/TGCGTTACGCTGG	R91C	255	1	0	0.002	0.000	0.000	0.005
MPJ6_U1A091[a]				Exon 1	135753	325	CATCTTCTGAAGA/GGATATTCTAGAA	R109G	255	1	0	0.002	0.000	0.000	0.005
MPJ6_U1A092[a]				Exon 1	135785	357	AATTATGAACAAT/CGTATCTTTGGCC	N119N	254	2	0	0.004	0.008	0.006	0.000
MPJ6_U1A093	rs12468274		O	Exon 1	135876	448	TTTGATGTGGTTT/CTAACAGACCCCG	L150L	195	54	7	0.133	0.133	0.142	0.125
MPJ6_U1A094	rs2011404		O	Exon 1	135899	471	CGTTAACCTCTGC/T[c]GGGGCGGTGCTG	C157C	251	5	0	0.010	0.008	0.011	0.009
MPJ6_U1A095	rs3732217	IMS-JST085727	O	Exon 1	136232	804	CTACCCCAGGCCG/AATCATGCCCAAC	P268P	195	54	7	0.133	0.133	0.142	0.125
MPJ6_U1A096[a]				Intron 1	136296	IVS1+1	CCACTATCTCAGG/TTCTGTATTGGTG		255	1	0	0.002	0.000	0.000	0.005
MPJ6_U1A097	rs2011219	IMS-JST085726	O	Intron 1	136338	IVS1+43	TTCCAGGCAAAAC/TACTTTTTAAAAA		195	54	7	0.133	0.133	0.142	0.125
MPJ6_U1A098[a]				Intron 1	136393	IVS1+98	ACTTATCTTTCCA/GAAGATTTTATTT		255	1	0	0.002	0.000	0.006	0.000
MPJ6_U1A099[a]				Intron 1	136396	IVS1+101	TATCTTTCCAAAG/TATTTTATTTTGG		253	3	0	0.006	0.008	0.006	0.005

[a]Novel variations detected in this study.
[b]The SNPs included in the PharmGKB database was shown as "O".
[c]T in the reference sequence.

A 127delA (43 fsX 22) (sense)

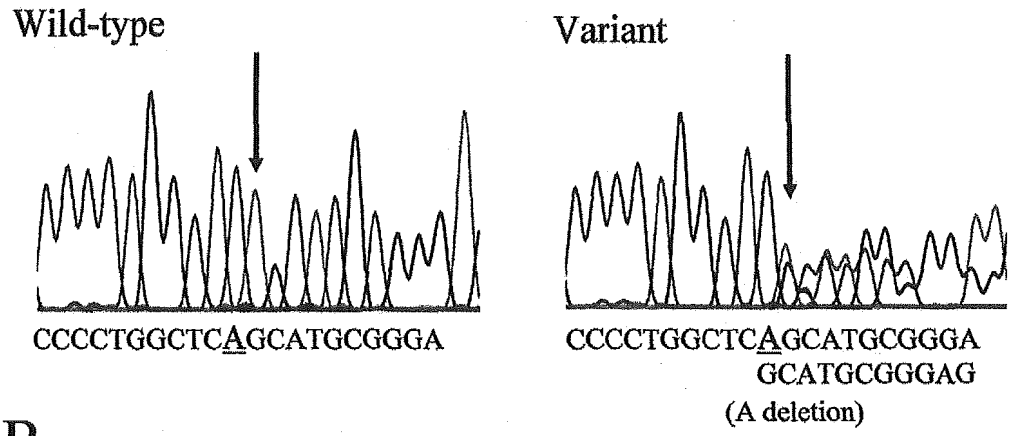

B 175delG (59 fsX 6) (sense)

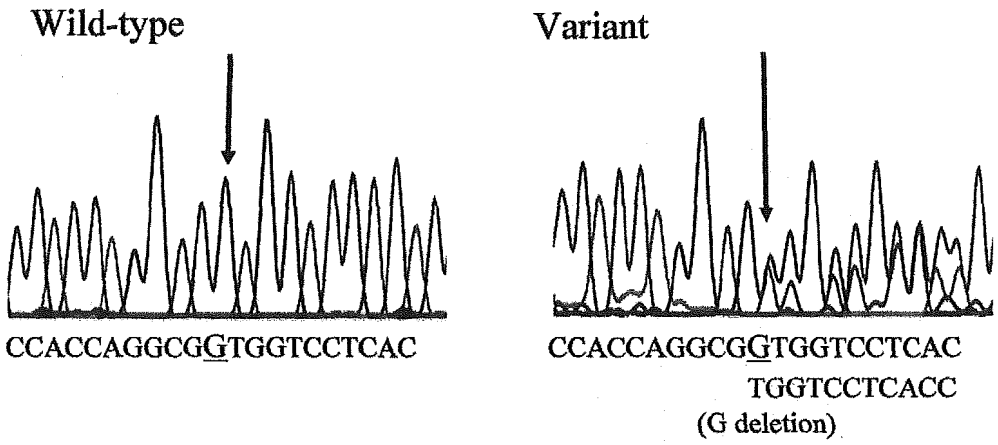

C 271C>T (Arg 91 Cys) (antisense)

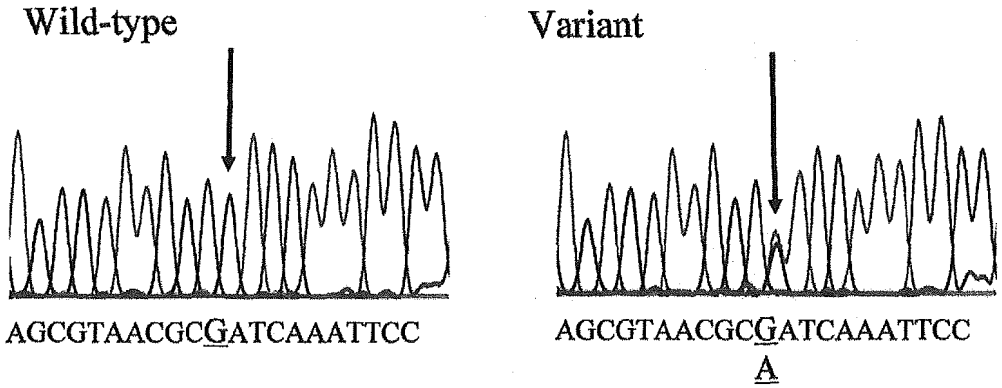

Fig. 1

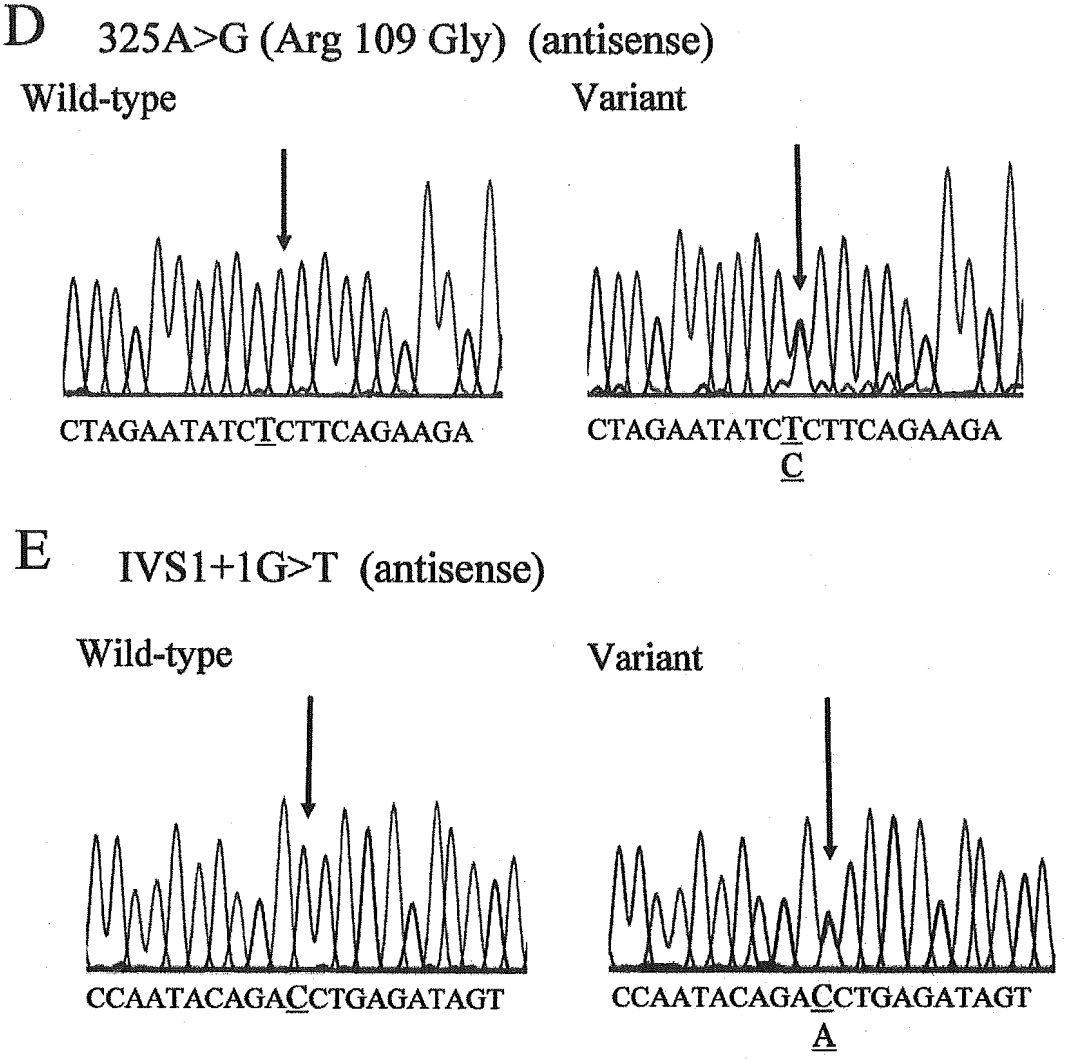

Fig. 1. The 4 novel genetic variations with amino acid substitutions and 1 splice donor site variation of human *UGT1A4*. (A) MPJ6_U1A087 (wild-type, 127A/A; variant, 127A/-). (B) MPJ6_U1A089 (wild-type, 175G/G; variant, 175G/-). (C) MPJ6_U1A090 (wild-type, 271C/C; variant, 271C/T). (D) MPJ6_U1A091 (wild-type, 325A/A; variant, 325A/G). (E) MPJ6_U1A096 (wild-type, IVS1+1G/G; variant, IVS1+1G/T). Arrows indicate the positions of the nucleotide changes.

the PCR on genomic DNA and sequencing the newly generated PCR products. Furthermore, the rare variations found in only one subject were confirmed by sequencing the PCR fragments produced by amplification with a high fidelity DNA polymerase KOD-Plus- (TOYOBO, Tokyo, Japan).

Linkage disequilibrium (LD) and haplotype analysis: Hardy-Weinberg equilibrium analysis and LD analysis were performed by SNPAlyze software (Dynacom Co., Yokohama, Japan). Pairwise LDs were shown in rho square (r^2) values. Some of the haplotypes were unambiguous from the subjects with homozygous SNPs at all sites or a heterozygous SNP at only one site. Separately, the diplotype configurations (a combination of haplotypes) were inferred by LDSUPPORT software, which determines the posterior probability distribution of the diplotype configuration for each subject based on the estimated haplotype frequencies.[11] The haplotypes were described as a number plus a small alphabetical letter.

Results and Discussion

UGT1A4 exon 1 and its flanking regions (from −286 bases upstream of the translational start site to 112 bases downstream of the end of exon 1) were sequenced from 256 Japanese subjects. Genbank accession number AF297093.1 was utilized for the reference sequence. Nineteen polymorphisms were detected, including 11 novel ones (2 were in the 5′-flanking region, 6 in exon 1, and 3 in the following intron) (**Table 2**). All of the allelic frequencies were in Hardy-Weinberg equilibrium ($p=$

0.13 or over). Since we did not find any significant differences in the frequencies of all the variations among three subject groups ($p>0.25$ by χ^2 test) and between two of the three groups ($p>0.13$ by χ^2 test or Fisher's exact test), the data for all subjects were analyzed as one group.

We found two novel nonsynonymous variations, 271C>T (R91C) and 325A>G (R109G), and two novel deletions, 127delA (43fsX22) and 175delG (59fsX6), as individual heterozygotes at a 0.002 frequency. Among them, 127delA (43fsX22) and 175delG (59fsX6) are the frameshift variations starting from codon 43 and 59, respectively, resulting in early stop codons at the 22nd (*i.e.* codon 65) and the 6th (*i.e.* codon 65) codons, respectively. It is most likely that these variations generate an immature protein that probably has null activity. The functional significance of 271C>T (R91C) and 325A>G (R109G) is currently unknown. Additionally, IVS1+1G>T, which was found at a frequency of 0.002, was located at a splice donor site and thus may lead to aberrant splicing (**Fig. 1**).

We also detected two known nonsynonymous SNPs, 31C>T (R11W) and 142T>G (L48V), at 0.012 and 0.129 frequencies, respectively. The frequency of 142T>G (L48V) was almost comparable to that of German Caucasians (0.09).[10] L48V was reported to lead to a partial decrease in glucuronidation of β-naphthylamine and benzidine, a marked decrease in the activity to *trans*-androsterone, and no activity toward dihydrotestosterone *in vitro*.[10] The functional significance of SNP 31C>T (R11W) has not been reported yet.

High linkage disequilibrium ($r^2 \geqq 0.89$) was observed among −219C>T, −163G>A, 142T>G (L48V), 448T>C (L150L), 804G>A (P268P), and IVS1+43C>T. A perfect linkage ($r^2=1$) was found between 175delG and 325A>G (R109G), but found in only one subject. The r^2 values were below 0.014 between the other pairs of polymorphisms. The SNP 70C>A (P24T), mostly linked with 142T>G (L48V) in German Caucasians,[10] was not detected in this study. Thus, it must be clarified whether the differences in the linkage of those SNPs may lead to the ethnic differences in the enzymatic activities of UGT1A4. A similar kind of ethnic difference has been found in the **1B* haplotype, which harbors the three linked SNPs in the 3′-untranslated region of UGT1A common exon 5 found in a Japanese population.[12] In Caucasian and African-American populations, this linkage of the 3 SNPs was not complete, especially in African-Americans.[13]

Using the detected SNPs, haplotype analysis was then performed (**Table 3**). Since *UGT1A4*2* [70C>A (P24T)] and **3* [142T>G (L48V)] were defined in AF465196 and AF465197 (Genbank accession numbers), respectively, the novel haplotypes with amino acid changes, frameshift variations, or splice donor site

Table 3. *UGT1A4* haplotypes in a Japanese population

Haplotype[b]	Nucleotide change[a]	−219 C>T	−217 T>G	−163 G>A	−36 G>A	30 G>A	31 C>T	127 delA	142 T>G	175 delG	271 C>T	325 A>G	357 T>C	448 T>C	471 C>T	804 G>A	IVS1 +1 G>T	IVS1 +43 C>T	IVS1 +98 A>G	IVS1 +101 G>T	Frequency
	Amino acid change					P10P	R11W	43fsX22	L48V	59fsX6	R91C	R109G	N119N	L150L	C157C	P268P					
*1	*1a																				0.818
	*1b																				0.010
	*1c																				0.008
	*1d																				0.006
	*1e																				0.004
	*1f																				0.004
	*1g																				0.002
	*1h																				0.002
	*1i																				0.002
*3	*3a																				0.123
	*3b																				0.002
*4	*4a																				0.012
*5	*5a																				0.002
*6	*6a																				0.002
*7	*7a																				0.002
*8	*8a																				0.002

[a] A of the translational start codon of *UGT1A4* is numbered 1. AF297093.1 was used as the reference sequence.
[b] The haplotypes were described as a number plus a small alphabetical letter.

variation, were assigned as haplotypes **4* to **8*. Several haplotypes were first unambiguously assigned by homozygous SNPs at all sites (**1a* and **3a*) or a heterozygous SNP at only one site (**1b*, **1d*-**1i*, **3b*, **4a*, and **8a*). Separately, we estimated the diplotype configuration (a combination of haplotypes) for each subject by LDSUPPORT software. The diplotype configurations of 256 subjects were inferred with probabilities (certainty) of 0.9998 or over, except for one subject. The additionally inferred haplotypes were **1c*, **5a*, **6a*, and **7a*. As for one subject with a low probability (who had heterozygous SNPs of −219C>T, −163 G>A, 31C>T, 142T>G, 448T>C, 804G>A, and IVS1+43C>T), the diplotype was determined by the cloning and sequencing of DNA fragments. One chromosome had haplotype **3a* (consisting of −219C>T, −163 G>A, 142T>G, 448T>C, 804G>A, and IVS1+43C>T) and the other had haplotype **4a* (31C>T). Moreover, the data obtained by cloning and sequencing analysis confirmed the presence of haplotypes **5a* [127delA (43fsX22) and 142T>G (L48V)], **6a* [175delG (59fsX6) and 325A>G (R109G)], and **7a* [−219C>T, −163G>A, 142T>G (L48V), 271C>T (R91C), 448T>C (L150L), 804G>A (P268P), and IVS1+43C>T] (**Table 3**). The most frequent haplotype was **1a* (frequency: 0.818), followed by **3a* (0.123), **4a* (0.012) and **1b* (0.010). The frequencies of the other haplotypes were less than 0.01. Since 325A>G (R109G) was linked with 175delG (59fsX6), the enzymatic activity of this haplotype (**6a*) is probably null. The other SNP, 271C>T confers the R91C substitution. In human UGT1A4, eight cysteine residues were located in the lumenal domain.[3,14] Though the disulfide-bond formation and its significance are not clear in the UGT1A4, it has been reported that the reduction of disulfide-bonds of rat UGT1A6 with dithiothreitol increases its enzymatic activity in the liver microsomes.[15] On the other hand, the alterations of several lumenal cysteines into serine residues seem to reduce the UGT1A6 activity when the mutant enzymes were expressed in COS cells.[15] The effect of additional cysteine residue at codon 91 in the UGT1A4 should be determined in the future.

In conclusion, we detected 19 polymorphisms, including 11 novel ones, in *UGT1A4* from a Japanese population. Using the detected polymorphisms, 16 haplotypes were identified. Our results provide fundamental and useful information for genotyping *UGT1A4* in the Japanese, and probably Asian populations.

Acknowledgments: We thank Ms. Chie Knudsen for her secretarial assistance.

References

1) Tukey, R. H. and Strassburg, C. P.: Human UDP-glucuronosyltransferase: Metabolism, Expression, and Disease. *Annu. Rev. Pharmacol. Toxicol.*, **40**: 581–616 (2000).
2) Mackenzie, P. I., Owens, I. S., Burchell, B., Bock, K. W., Bairoch, A., Belanger, A., Fournel-Gigleux, S., Green, M., Hum, D. W., Iyanagi, T., Lancet, D., Louisot, P., Magdalou, J., Chowdhury, J. R., Ritter, J. K., Schachter, H., Tephly, T. R., Tipton, K. F. and Nebert, D. W.: The UDP glycosyltransferase gene superfamily: recommended nomenclature update based on evolutionary divergence. *Pharmacogenetics*, **7**: 255–269 (1997).
3) Radominska-Pandya, A., Czernik, P. J. and Little, J. M.: Structural and functional studies of UDP-glucuronosyltransferases. *Drug Metab. Rev.*, **31**: 817–899 (1999).
4) Strassburg, C. P., Kneip, S., Topp, J., Obermayer-Straub, P., Barut, A., Tukey, R. H. and Manns, M. P.: Polymorphic gene regulation and interindividual variation of UDP-glucuronosyltransferase activity in human small intestine. *J. Biol. Chem.*, **275**: 36164–36171 (2000).
5) Ockenga, J., Vogel, A., Teich, N., Keim, V., Manns, M. P. and Strassburg, C. P.: UDP glucuronosyltransferase (UGT1A7) gene polymorphisms increase the risk of chronic pancreatitis and pancreatic cancer. *Gastroenterology*, **124**: 1802–1808 (2003).
6) Green, M. D. and Tephly, T. R.: Glucuronidation of amines and hydroxylated xenobiotics and endobiotics catalyzed by expressed human UGT1.4 protein. *Drug Metab. Dispos.*, **24**: 356–363 (1996).
7) Nakajima, M., Tanaka, E., Kobayashi, T., Ohashi, N., Kume, T. and Yokoi, T.: Imipramine *N*-glucuronidation in human liver microsomes: biphasic kinetics and characterization of UDP-glucuronosyltransferase isoforms. *Drug Metab. Dispos.*, **30**: 636–642 (2002).
8) Nakajima, M., Tanaka, E., Kwon, J. T. and Yokoi, T.: Characterization of nicotine and cotinine *N*-glucuronidations in human liver microsomes. *Drug Metab. Dispos.*, **30**: 1484–1490 (2002).
9) Kaku, T., Ogura, K., Nishiyama, T., Ohnuma, T., Muro, K. and Hiratsuka, A.: Quaternary ammonium-linked glucuronidation of tamoxifen by human liver microsomes and UDP-glucuronosyltransferase 1A4. *Biochem. Pharmacol.*, **67**: 2093–2102 (2004).
10) Ehmer, U., Vogel, A., Schutte, J. K., Krone, B., Manns, M. P. and Strassburg, C. P.: Variation of hepatic glucuronidation: Novel functional polymorphisms of the UDP-glucuronosyltransferase UGT1A4. *Hepatology*, **39**: 970–977 (2004).
11) Kitamura, Y., Moriguchi, M., Kaneko, H., Morisaki, H., Morisaki, T., Toyama, K. and Kamatani, N.: Determination of probability distribution of diplotype configuration (diplotype distribution) for each subject from genotypic data using the EM algorithm. *Ann. Hum. Genet.*, **66**: 183–193 (2002).
12) Sai, K., Saeki, M., Saito, Y., Ozawa, S., Katori, N.,

Jinno, H., Hasegawa, R., Kaniwa, N., Sawada, J., Komamura, K., Ueno, K., Kamakura, S., Kitakaze, M., Kitamura, Y., Kamatani, N., Minami, H., Ohtsu, A., Shirao, K., Yoshida, T. and Saijo, N.: UGT1A1 haplotypes associated with reduced glucuronidation and increased serum bilirubin in irinotecan-administered Japanese patients with cancer. *Clin. Pharmacol. Ther.*, **75**: 501–515 (2004).

13) Kaniwa, N., Kurose, K., Jinno, H., Tanaka-Kagawa, T., Saito, Y., Saeki, M., Sawada, J., Tohkin, M. and Hasegawa, R.: Racial variability in haplotype frequencies of UGT1A1 and glucuronidation activity of a novel SNP 686C>T (P229L) found in an African-American. *Drug Metab. Dispos.*, in press.

14) Ritter, J. K., Crawford, J. M. and Owens, I. S.: Cloning of two human liver bilirubin UDP-glucuronosyltransferase cDNAs with expression in COS-1 cells. *J. Biol. Chem.*, **266**: 1043–1047 (1991).

15) Ikushiro, S., Emi, Y. and Iyanagi, T.: Activation of glucuronidation through reduction of a disulfide bond in rat UDP-glucuronosyltransferase 1A6. *Biochemistry*, **41**: 12813–12820 (2002).

Interaction magnitude, pharmacokinetics and pharmacodynamics of ticlopidine in relation to *CYP2C19* genotypic status

Ichiro Ieiri[a], Miyuki Kimura[b], Shin Irie[b], Akinori Urae[b], Kenji Otsubo[a] and Takashi Ishizaki[c]

Objectives The aim of this study was to investigate the impact of *CYP2C19* polymorphism on the extent of the interaction and on the pharmacokinetics and pharmacodynamics of ticlopidine.

Methods Homozygous (hmEMs) and heterozygous extensive metabolizers (htEMs), and poor metabolizers (PMs, $n=6$ each) took an oral dose (20 mg) of omeprazole. After a 1-week washout period, each subject received ticlopidine (200 mg) for 8 days, and ticlopidine pharmacokinetics were studied on days 1 and 7. On day 8, omeprazole was given again and its kinetic disposition was compared with that in the first dose. ADP-induced platelet aggregation was measured as a pharmacodynamic index.

Results In contrast to the PMs, whose mean kinetic parameters were not altered by the repeated dosings of ticlopidine, an eight- to 10-fold increase in the mean AUC ratio of omeprazole to 5-hydroxyomeprazole was observed in both the EM groups. No significant intergenotypic differences in the pharmacokinetic parameters of ticlopidine were observed, although the accumulation ratio tended to be greater in hmEMs than in PMs (2.4 ± 0.2 versus 1.7 ± 0.2). A significantly positive correlation ($P=0.031$) was observed between the individual percent inhibition of platelet aggregation and AUC_{0-24} of ticlopidine regardless of the *CYP2C19* polymorphism.

Conclusions Ticlopidine is a potent inhibitor for CYP2C19 and may be associated with the phenocopy when CYPC19 substrates are co-administered to EMs. Whether and to what extent CYP2C19 would be involved in the metabolism of ticlopidine remain unanswered from the present in-vivo study. *Pharmacogenetics and Genomics* 15:851–859

Pharmacogenetics and Genomics 2005, 15:851–859

Keywords: ticlopidine, CYP2C19, pharmacogenetics, pharmacokinetics, pharmacodynamics

[a]Department of Hospital Pharmacy, Faculty of Medicine, Tottori University, Yonago, Japan, [b]Kyushu Clinical Pharmacology Research Clinic, Fukuoka, Japan and [c]Department of Clinical Pharmacology and Pharmacy, Teikyo Heisei University School of Pharmaceutical Science, Ichihara, Japan.

Correspondence and requests for reprints to Ichiro Ieiri, PhD, Department of Hospital Pharmacy, Faculty of Medicine, Tottori University, Nishi-machi 36-1, Yonago, 683-8504, Japan.
Fax: +81-859-34-8087; e-mail: ieiri-ttr@umin.ac.jp

Received 8 April 2005 Accepted 23 July 2005

Introduction

Ticlopidine is the first of the thienopyridine antiplatelet agents, known as adenosine diphosphate (ADP) receptor antagonists [1]. Studies have demonstrated that ticlopidine reduces the risk of thrombotic events in patients with stroke [2,3], and is effective for the treatment of unstable angina [4], myocardial infarction [5], and intermittent claudication [6]. Furthermore, in combination with aspirin, ticlopidine reduces thrombotic complications following coronary stent placement [7–9].

The pharmacokinetic behavior of ticlopidine has been mainly investigated in Caucasian subjects [10,11]. Although up to 90% of an oral dose is absorbed, ticlopidine is extensively metabolized in the liver, resulting in the formation of more than 13 metabolites, of which the 2-keto derivative is reported to inhibit platelet aggregation in rats [10]. Plasma ticlopidine concentrations [e.g., the peak concentration (C_{max}) and the area under the plasma concentration–time curve (AUC)] increase by approximately three-fold on repeated twice-daily dosings over 2 to 3 weeks [10,11], suggesting that an accumulation or saturation in the metabolism may occur during a repeated administration.

Studies *in vitro* and *in vivo* have documented that ticlopidine is an inhibitor of cytochrome P450 (CYP) enzymes (e.g., CYP2B6, 2C19, 2D6 and/or 2C9) [12–17]. Ko *et al.* [15] and Ha-Duong *et al.* [16] have reported that ticlopidine is an inhibitor of human CYP2C19, whereas Lopez-Garcia *et al.* [17] have reported that thiophene derivatives such as tienilic acid are mechanism-based inhibitors of yeast-expressed human liver CYP2C9. A more recent study by Richter *et al.* [13] has indicated that ticlopidine is a mechanism-based inhibitor of CYP2B6, as well as shows an inhibitory effect against CYP2C19.

1744-6872

Tateishi *et al.* [18] have shown that ticlopidine inhibits the in-vivo activity of CYP2C19 using omeprazole as a model substrate in small number ($n = 6$) of *CYP2C19*-genotyped Japanese extensive, but not poor, metabolizers. In addition, two in-vitro studies using recombinant human liver CYPs have demonstrated that CYP2C19 and CYP3A4 are involved in the metabolism of ticlopidine [16,19].

With this background in mind, we designed the present study (1) to confirm the in-vivo inhibitory effect of ticlopidine on the metabolism of omeprazole mediated via CYP2C19 (i.e., omeprazole 5-hydroxylation) in 18 Japanese subjects including six poor metabolizers, and (2) to assess the pharmacokinetics and dynamics of ticlopidine administered in single and multiple doses in the same 18 *CYP2C19*-genotyped subjects. These two study aims are justified because it is possible that ticlopidine itself is a substrate of CYP2C19 and CYP3A4 as it undergoes extensive hepatic metabolism [10,16,19], although it is reasonable to suspect that ticlopidine inhibits multiple CYP isoforms including CYP2B6, 2C19, 2C9, 1A2 and 3A [12–18].

Methods

Subjects

Eighteen unrelated healthy volunteers identified as Japanese by lineage (age, 20~33 years; weight, 52.5~75.9 kg; body mass index; 18.5~24.9 kg/m^2) were enrolled. Subjects were genotypically classified into the following three groups on the basis of a PCR–restriction fragment length polymorphism analysis for *CYP2C19*: homozygous (*CYP2C19*1/*1*) extensive metabolizers (hmEMs, $n = 6$), heterozygous (*CYP2C19*1/*2*) extensive metabolizers (htEMs, $n = 6$), and poor metabolizers (PMs, *CYP2C19*2/*2*, $n = 4$ and *CYP2C19*2/*3*, $n = 2$). None had taken any drugs for at least 1 week before the study. Each subject was physically normal and had no antecedent history of significant medical illness or hypersensitivity to any drugs. The subjects' health status was judged to be normal on the basis of a physical examination with hepatic function screening, a complete blood cell count, serum creatinine analysis, urinalysis, a platelet aggregation test, and an electrocardiogram before the study. The study subjects included nine nonsmokers and nine smokers (< 10 cigarettes per day). Smokers were not allowed to smoke during the period of hospitalization. All subjects were required to abstain from alcohol 2 days before the drug administration and during the period of hospitalization. The subjects were served standard meals on the study days. To assess the safety of the drugs studied, we evaluated spontaneous adverse events reports and conducted electrocardiogram recordings, laboratory safety evaluations (hematology, blood chemistry, and urinalysis), and immunological tests (antinuclear antibody, and anti-liver–kidney microsome antibody type 1 and type 2), before and after the trial phases. The study protocol had been approved in advance by the ethics review board of Kyushu Clinical Pharmacology Research Clinic, Fukuoka, Japan, and each subject gave their written informed consent before the study.

Study protocol

The protocol is summarized in Fig. 1. The participants came to the clinical research site on the day before the study, and after an overnight fast, each subject was administered a single oral 20-mg dose of omeprazole (Omepral, AstraZeneca Co. Ltd., Osaka, Japan) with 150 ml of water (day 0). Food was given 4 h after the ingestion of omeprazole. After a wash-out period of 1 week, each subject was administered a once-daily 200-mg dose of ticlopidine (two tablets of 100 mg Panaldine, Daiichi Pharmaceutical Co. Ltd., Tokyo, Japan) with 150 ml of water at 8 am after a standard breakfast on day 1

Fig. 1

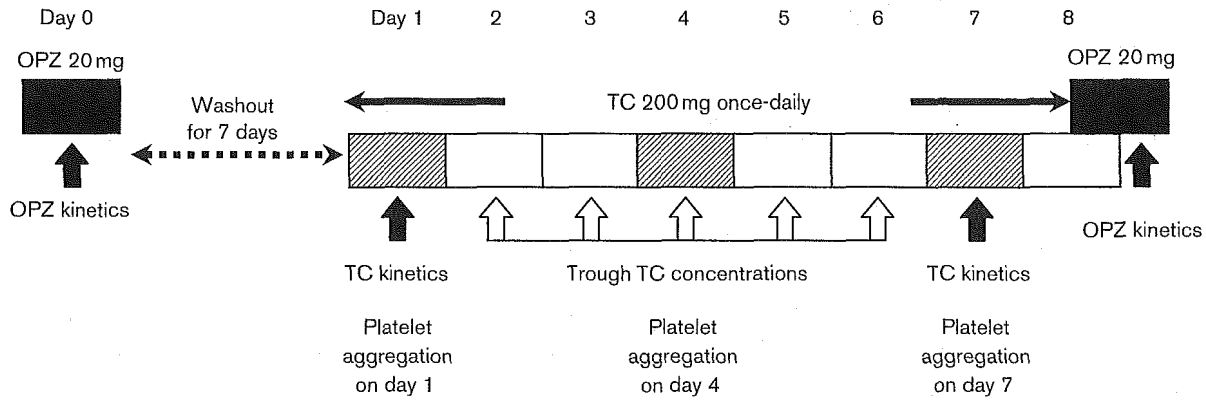

Schema of the study design. Subjects received a single dose of omeprazole (OPZ). After a 7-day washout period, they received a once-daily 200-mg dose of ticlopidine (TC) for 8 days. On day 8, an oral 20-mg dose of omeprazole was administered again at 1 h after the administration of the oral 200-mg dose of ticlopidine.

through day 8. Ticlopidine pharmacokinetics were studied on days 1 and 7. On day 8, an oral 20-mg dose of omeprazole was administered at 1 hour after the administration of the oral 200-mg dose of ticlopidine. Venous blood samples (4 ml each) for determining omeprazole, 5-hydroxyomeprazole and ticlopidine concentrations were obtained just before and 0.5, 1, 2, 3, 4, 6, 8, 12 and 24 h after the administration. In order to assess the accumulation of ticlopidine, trough concentrations were measured just before the ticlopidine administration on day 2 through day 8. The plasma samples were immediately separated after centrifugation and stored at −20°C until analyzed.

Platelet aggregation

Blood samples (4.5 ml each) were obtained with a 21-gauge needle by direct venepuncture and drawn into vacuum tubes containing sodium citrate for measuring platelet aggregation. The vacuum tube was filled to capacity and gently inverted five times to ensure complete mixing of the anticoagulant, and then centrifuged at 90*g* for 10 minutes at 22°C in order to obtain platelet-rich plasma (PRP). The rest of the samples were centrifuged at 1630*g* for 10 minutes at 22°C in order to obtain platelet-poor plasma (PPP). Platelet aggregation was determined five times during the study period; at the screening visit, on days 1, 4 and 7 of the ticlopidine dosings, and at 14 to 20 days after discharge from the clinic for the monitoring of platelet recovery. All samples were taken immediately before lunch. Platelet aggregation was measured according to the method of Born [20] with a PA-200 instrument (Kowa Co. Ltd., Tokyo, Japan). Adenosine diphosphate (ADP, MC Medical Co. Ltd., Tokyo, Japan) was used as an aggregating agent. The extent of platelet aggregation was evaluated by measuring the maximal extension of the aggregation curve 5 min after the addition of 5 μM ADP.

Analytical methods

Plasma concentrations of ticlopidine, omeprazole, and 5-hydroxyomeprazole were measured using the respective validated liquid chromatography/mass spectrometry/mass spectrometry (LC/MS/MS) methods as described below.

For the ticlopidine analysis 10 μl of methanol and 20 μl of internal standard (mianserin, 1000 ng/ml in methanol) were added to 0.1 ml of plasma. The analytes were extracted into *n*-hexane (6 ml) from an alkaline pH (0.2 ml of 1 mol/l NaOH), then back-extracted into 0.1 M HCl (0.5 ml). Aliquots (10 μl) were injected into the LC/MS/MS system which consisted of an API3000 system (AB/MDS Sciex, Foster City, California, USA) and Agilent 1100 HPLC system (Agilent Technologies, Palo Alto, California, USA).

For the omeprazole and 5-hydroxyomeprazole analyses, 0.1 ml of plasma was mixed with 10 μl of methanol, 10 μl of a methanolic solution with 1000 ng/ml of phenacetin as an internal standard and 0.1 M phosphate buffer (pH 7.5, 0.6 ml), and then applied to a solid-phase extraction cartridge (Oasis HLB, 30 mg/ml, Waters, Milford, Massachusetts, USA). These cartridges were then washed with 1.0 ml of 15% methanol, and the sample was eluted with 3 ml of methanol. The eluate was evaporated to dryness under a gentle stream of nitrogen at 40°C, and the residue was reconstituted in 0.2 ml of a high pressure liquid chromatography mobile phase consisting of 10 mM ammonium formate (pH 8.5)/acetonitrile (75:25 [vol/vol]). After sonication and centrifugation, the supernatant was filtered through Ultrafree (0.45 μm, PTFE, Millipore, Bedford, Massachusetts, USA), and an aliquot of the filtrate (5 μl) was injected into the LC/MS/MS system.

Chromatographic separation of ticlopidine was performed on a Luna C18(2) column (3 μm, 2.0 × 50 mm; Phenomenex, Torrance, California, USA) with a Security Guard C18(ODS) column (2.0 × 4 mm, Phenomenex) at 30°C using a mobile phase consisting of 0.1% acetic acid/acetonitrile (80:20 [vol/vol]) at a flow rate of 0.20 ml/min. Omeprazole and 5-hydroxyomeprazole were separated on a Xterra MS C18 column (3.5 μm, 2.1 × 50 mm; Waters) at 40°C using a mobile phase consisting of 10 mM ammonium formate (pH 8.5)/acetonitrile (75:25 [vol/vol]) at a flow rate of 0.2 ml/min.

Detection was carried out in the electrospray ionization (TurboIonSpray) mode with multiple reaction monitoring using the API3000 system. The monitor ions were *m/z* 264→154 (Q1→Q3) [−25 eV] for ticlopidine, *m/z* 265→208 (Q1→Q3) [−29 eV] for mianserin, *m/z* 346→198 (Q1→Q3) [−17 eV] for omeprazole, *m/z* 362→214 (Q1→Q3) [−15 eV] for 5-hydroxyomeprazole, and *m/z* 180→138 (Q1→Q3) [−23 eV] for phenacetin. Calibration was performed with blank plasma samples spiked with the respective standard substances. Calibration curves were constituted from the ratio of peak area relative to the internal standard using Analyst version 1.1 (AB/MDS Sciex) with weighted ($1/x$) linear regression in a range of 0.5–500 ng/ml for ticlopidine and with weighted ($1/x$) quadratic regression in a range of 5–500 ng/ml for omeprazole and 5-hydroxyomeprazole. The accuracy in four of six quality control samples prepared using blank human plasma was within ± 20%. The plasma samples exceeding the quantitation range were diluted 10-fold with blank human plasma.

Pharmacokinetic analysis

Peak concentrations (C_{max}) and time of maximum concentration (T_{max}) were obtained directly from the data. Pharmacokinetic analysis was performed in a model-independent manner, and non-compartmental kinetic parameters were calculated using standard methods. The area under the observed concentration–time curve from

time 0 to 24 h (AUC_{0-24}) was calculated with the linear trapezoidal rule. The elimination rate constant (k_e) was estimated using the least regression analysis from the terminal post-distribution phase of the concentration-time curve. The terminal half-life ($t_{1/2}$) was calculated by dividing 0.693 by the elimination rate constant. The AUC from 0 h to infinity ($AUC_{0-\infty}$) was calculated as follows: $(AUC_{0-\infty}) = (AUC_{0-24}) + C_t/k_e$, in which C_t represents the last measured time point concentration. To assess the possibility of accumulation of ticlopidine with multiple dosings, the accumulation ratio, the AUC_{0-24} ratio of day 7 to day 1, was calculated.

Statistical analysis

The numerical values are given as the mean ± SE. Statistical differences in mean pharmacokinetic parameters for omeprazole, 5-hydroxyomeprazole and ticlopidine among the three *CYP2C19* genotype groups were determined by use of one-way ANOVA followed by the Scheffé multiple comparison test. Statistically significant differences in pharmacodynamic parameters among the three genotype groups were determined by use of the Mann–Whitney *U* test. Statistical differences in mean pharmacokinetic parameters of ticlopidine observed on days 1 and 7, and in the omeprazole/5-hydroxyomeprazole ratio before and after the multiple ticlopidine dosings were evaluated with the paired *t*-test. For correlation between % inhibition of platelet aggregation and AUC of ticlopidine, the Spearman rank correlation test was applied. All *P* values were two-sided; $P < 0.05$ was considered statistically significant.

Results

No clinically undesirable signs and symptoms possibly attributed to the administration of ticlopidine and/or omeprazole were recognizable throughout the study. According to the protocol, all subjects completed the study successfully.

Omeprazole pharmacokinetics with and without ticlopidine co-administration in relation to *CYP2C19* genotypic status

Plasma concentrations of omeprazole on day 0 were higher and those of 5-hydroxyomeprazole were lower in PMs compared with those in the two EM groups (Fig. 2a, b). However, these intergenotypic differences almost disappeared on the eighth day of ticlopidine administration (Fig. 2c, d). As observed from the change in AUC and in elimination half-life, the inhibition of omeprazole metabolism was significant in both the EM groups (Table 1). After the administration of ticlopidine for 1 week, the AUC values of omeprazole and 5-hydroxyomeprazole in the EMs were increased by three to six times and reduced by approximately 40%, respectively, resulting in the values similar to those in the PMs (Table 1). The $AUC_{0-\infty}$ ratio of omeprazole to 5-hydroxyomeprazole showed a significant reduction of 5-hydroxyomeprazole production in both the EM groups; in contrast, no significant changes were observed in PMs (Fig. 3).

Ticlopidine pharmacokinetics in relation to *CYP2C19* genotypic status

The mean plasma concentration–time curves of ticlopidine in relation to *CYP2C19* status on the first and seventh days of ticlopidine dosings is shown in Fig. 4. The pharmacokinetic parameters of ticlopidine are summarized in Table 2. Statistically significant intergenotypic differences in the mean pharmacokinetic parameters of ticlopidine were not observed on either of the study days. However, the mean (± SE) accumulation ratio of ticlopidine, the AUC_{0-24} ratio of day 7 to day 1, in the hmEMs, htEMs, and PMs was 2.4 ± 0.2, 2.0 ± 0.3, and 1.7 ± 0.1, respectively. Although the difference did not reach the level of significance, the accumulation ratio tended to be greater in the hmEM subjects compared with the htEM or PM subjects. The mean trough concentration data of ticlopidine from day 2 to day 8 are also shown in Fig. 4. Similar to the accumulation ratio, the mean trough levels tended to be higher in the hmEM subjects compared with the PM subjects, and the htEM subjects had the values between those in hmEM and PM subjects throughout the study period (see the inset of Fig. 4).

Pharmacodynamics of ticlopidine versus *CYP2C19* status

As a pharmacodynamic assessment of ticlopidine, ADP-induced platelet aggregation was measured on the first, fourth and seventh days of the 8-day dosing period and compared with the baseline values in the different *CYP2C19* genotypic groups. The mean maximum percentage values for ADP-induced platelet aggregation relative to the baseline values on the first, fourth and seventh post-dose days were: 77.3 ± 11.5, 55.0 ± 15.3 and 46.5 ± 14.3 in the hmEMs, 75.8 ± 8.7, 50.0 ± 7.7 and 42.5 ± 5.5 in the htEMs, and 77.0 ± 14.4, 59.8 ± 15.4 and 55.0 ± 17.2 in the PMs, respectively. Thus, the mean percentage inhibition of ADP-induced platelet aggregation on the first versus the fourth and seventh post-dose days increased with the repeated doses, irrespective of *CYP2C19* status: 29.5 ± 12.4% and 40.4 ± 12.4% in the hmEMs, 33.7 ± 10.6% and 43.7 ± 6.8% in the htEMs, and 21.3 ± 18.0% and 28.4 ± 17.2% in the PMs. The mean maximum and percentage inhibition values for ADP-induced platelet aggregation observed throughout the treatment period did not differ significantly among the genotypic groups.

The relationship between the individual percent inhibition of platelet aggregation and AUC_{0-24} values observed on the seventh day of ticlopidine dosing is shown in Fig. 5. The AUC_{0-24} of ticlopidine is significantly ($P = 0.031$) correlated with the percent inhibition of

Fig. 2

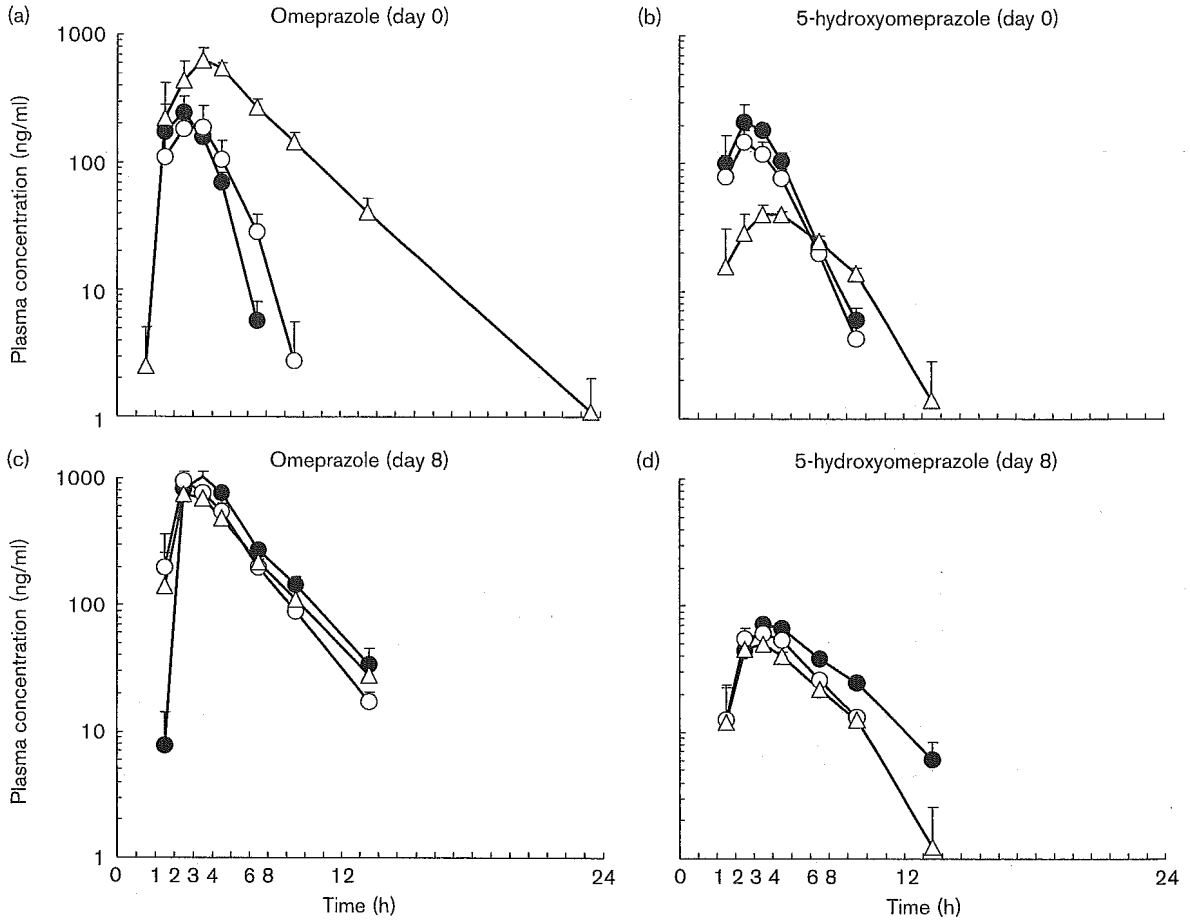

The mean plasma concentrations of omeprazole and 5-hydroxyomeprazole among homozygous extensive metabolizers (hmEMs, closed circles), heterozygous extensive metabolizers (htEMs, open circles) and poor metabolizers (PMs, triangles) after a single oral 20-mg dose of omeprazole before (day 0) and after (day 8) the concomitant intake of 200 mg/day ticlopidine.

Table 1 Pharmacokinetic data for omeprazole and 5-hydroxyomeprazole in the *CYP2C19* genotypic groups

	Before ticlopidine (day 0)			After ticlopidine (day 8)		
	Homozygous EMs ($n=6$)	Heterozygous EMs ($n=6$)	PMs ($n=6$)	Homozygous EMs ($n=6$)	Heterozygous EMs ($n=6$)	PMs ($n=6$)
Omeprazole						
C_{max} (ng/ml)	383.0 ± 67.7	289.8 ± 71.0	889.0 ± 71.7**	1143.3 ± 100.9††	978.1 ± 62.1††	839.1 ± 60.9
T_{max} (h)	2.0 ± 0.4	2.3 ± 0.4	2.7 ± 0.4	2.8 ± 0.3	2.7 ± 0.3	2.5 ± 0.2
$T_{1/2}$ (h)	0.7 ± 0.1	0.7 ± 0.1	2.1 ± 0.2**	1.8 ± 0.2†	1.6 ± 0.1	1.9 ± 0.2
$AUC_{0-\infty}$ (ng·h/ml)	646.7 ± 110.8	653.5 ± 159.5	3284.4 ± 288.8***	4023.2 ± 255.2†††	3271.8 ± 300.5†††	3208.9 ± 252.6
5-hydroxyomeprazole						
C_{max} (ng/ml)	325.7 ± 43.5	183.4 ± 21.6	53.5 ± 7.7***	76.3 ± 6.6†††	71.5 ± 2.7**	54.1 ± 3.9
T_{max} (h)	2.2 ± 0.3	2.3 ± 0.4	3.2 ± 0.7	3.0 ± 0.4	2.7 ± 0.3	2.3 ± 0.3
$T_{1/2}$ (h)	1.0 ± 0.1	1.0 ± 0.1	2.4 ± 0.2**	2.8 ± 0.4††	2.1 ± 0.1††	2.5 ± 0.3
$AUC_{0-\infty}$ (ng·h/ml)	692.4 ± 40.5	494.5 ± 62.5	248.6 ± 18.9**	419.6 ± 22.9††	312.5 ± 14.3†	271.7 ± 7.8
AUC ratio*	0.9 ± 0.1	1.3 ± 0.3	13.4 ± 0.7	9.7 ± 0.7†††	10.6 ± 1.0†††	11.8 ± 0.9

Data are the mean ± SE.
AUC ratio: $AUC_{0-\infty}$ ratio of omeprazole to 5-hydroxyomeprazole (i.e., omeprazole hydroxylation index).
$^{*}P<0.05$ (versus EMs); $^{**}P<0.01$ (versus EMs); $^{***}P<0.001$ (versus EMs); $^{\dagger}P<0.05$ (versus before ticlopidine); $^{\dagger\dagger}P<0.01$ (versus before ticlopidine); $^{\dagger\dagger\dagger}P<0.001$ (versus before ticlopidine).